energy&fuels

Article

pubs.acs.org/EF

Evolution of NO_x Precursors during Rapid Pyrolysis of Coals in CO_2 Atmosphere

Xiangpeng Li, Shihong Zhang,* Wei Yang, Yi Liu, Haiping Yang, and Hanping Chen

State Key Laboratory of Coal Combustion, Huazhong University of Science and Technology, Luoyu Road 1037, Hongshan District, Wuhan, Hubei 430074, People's Republic of China

ABSTRACT: To understand the effect of CO_2 on fuel N evolution during rapid coal pyrolysis, pyrolysis/gasification of EH lignite and HL bituminous coal were carried out in a suspension-bed reactor under N_2 or CO_2 atmosphere. The chemical and physical structures of the chars were measured by Fourier transform infrared spectrometry and X-ray diffractometry. The results show that higher temperature is favorable for the evolution of HCN and NH_3. Thermally stable quaternary N is believed to be the important intermediate for the formation of NH_3. The presence of CO_2 can promote HCN and NH_3 generation through the creation of H radicals and the cracking of N-containing groups. However, the HCN yields of HL coal pyrolyzed in CO_2 at 700 and 800 °C are lower than that in N_2, and a similar result was obtained for EH coal at 1000 °C, which are caused by the blocking effect of CO_2 and the reaction of HCN with CO_2, respectively. Structural analyses of the chars show that in the initial stage of coal pyrolysis/gasification, CO_2 can suppress the polymerization of aliphatic chains and more H is retained as $-CH_2$ or $-CH_3$ in chars. Subsequently, gasification of CO_2 with the rich aliphatic chains is helpful to produce abundant H radicals for the formation of NH_3.

1. INTRODUCTION

Oxy-fuel combustion, in which nitrogen is replaced by highly concentrated CO_2 from flue gas by flue gas recycle, is considered a promising and near-term technology for CO_2 reduction in coal-fired power plants.[1,2] Because of their different physical and chemical characteristics, the replacement of N_2 by CO_2 changes the combustion conditions considerably, which affects the combustion behaviors and pollutant emissions, including NO_x formation and evolution of its precursors during pyrolysis.[2−4]

Pyrolysis is the preliminary process of coal combustion and plays a significant role in the subsequent combustion process. During coal pyrolysis, NO_x precursors (mainly HCN and NH_3) are produced from fuel N and are then oxidized to NO_x, which is a significant gas pollutant that causes acid rain and photochemical smog. Hence, it is essential to study the fate of fuel N in oxy-fuel combustion and the effects of CO_2 on the generation of HCN and NH_3 during coal pyrolysis.

Ohtsuka et al.[3] studied the distribution of N_2, NH_3, and HCN during slow heating rate pyrolysis of a sub-bituminous coal in He and gasification in 10% CO_2 + He balance. The results showed that CO_2 suppressed the release of HCN and NH_3, which might be attributed to the reaction between HCN (or NH_3) and CO_2. Feng et al.[4] indicated that volatiles were the main source of HCN and NH_3 formation. The optimum temperature for NH_3 generation in CO_2 gasification was 800 °C, and the formation of HCN was almost unrelated to the gasification of H_2O or CO_2. Li et al.[5] found that, during the initial stage of pyrolysis, NH_3 and HCN formation was inhibited by chemisorption of CO_2 on the nascent char surface, which could consume H radicals or block access of the H radicals to the N sites. However, more H radicals were generated by char CO_2 gasification, enhancing the formation of NH_3 but not leading to HCN formation in the late stage of pyrolysis. Duan et al.[6] found that char CO_2 gasification was evident at temperatures above 480 °C and could promote the conversion of char N to HCN; however, no NH_3 was detected. In another study, they also found that a CO_2 atmosphere suppressed the formation of NH_3 and enhanced HCN production as a result of the gasification effect.[7]

Most studies are focused on slow pyrolysis; however, the pyrolysis process in industrial combustion is extremely fast and the effects of CO_2 on the generation of NO_x precursors from fuel N under this condition remain unclear. Here, the effects of CO_2 on HCN and NH_3 generation were investigated by rapid pyrolysis experiments in a suspension-bed reactor. Furthermore, because the formation of HCN and NH_3 are closely associated with hydrogen in chars, the chemical and physical structures of the resultant solid chars were investigated using Fourier transform infrared (FTIR) spectrometry and X-ray diffractometry (XRD) to reveal the effect of CO_2 on H functional groups and N-containing gas evolution.

2. EXPERIMENTAL SECTION

2.1. Samples. On the basis of different coal ranks, Ejinaoer (EH) coal and Huangling (HL) coal were chosen as coal samples. EH is a high-volatile and low-ash lignite from Xilinguole League of Inner Mongolia, and HL is a bituminous coal with high ash content from Huangling City of Shanxi Province. All the samples were crushed and sieved to 0.45−0.6 mm, dried in an oven at 55 °C for 4 h to remove external moisture, and then sealed as experimental samples. The proximate and ultimate analyses of the samples are listed in Table 1. EH is a low-rank coal containing a high level of oxygen, whereas HL is an easy-coking coal. Because of its well-developed pore structures and high reactivity, EH char is more reactive with CO_2 than HL char.

2.2. Pyrolysis Experiments. The pyrolysis experiments were performed in a suspension-bed reactor at different temperatures, as

Received: July 2, 2015
Revised: October 12, 2015
Published: October 13, 2015

DOI: 10.1021/acs.energyfuels.5b01509
Energy Fuels 2015, 29, 7474−7482

Table 1. Proximate and Ultimate Analyses of Coals[a]

	proximate analysis (wt %)				ultimate analysis (wt %)				
sample	M_{ad}	V_d	A_d	FC_d	C_d	H_d	N_d	S_d	O_d[b]
EH	14.15	38.96	11.27	49.77	61.24	4.65	0.94	0.45	21.45
HL	2.93	25.96	30.01	44.03	55.24	3.95	0.68	2.04	8.08

[a]ad, air-dried basis; d, dry basis. [b]By difference.

shown in Figure 1. The reactor is made of quartz, with an inner diameter of 50 mm and a height of 1000 mm. An upper conical section

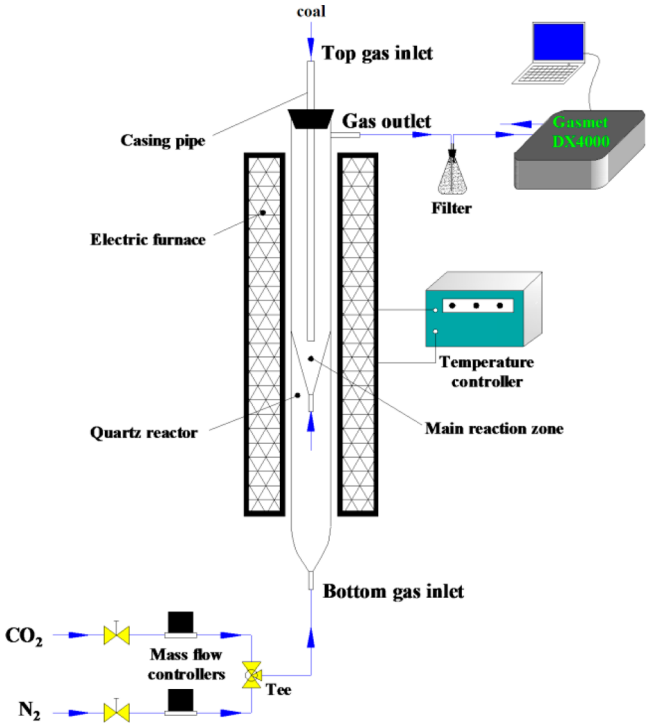

Figure 1. Scheme of the suspension-bed reactor system.

in the middle of the reactor divides the reactor into three sections: bottom, conical, and upper. The bottom section provides a preheating zone whereas the conical section is the main reaction zone, where coal particles are suspended by upward gas flow. The reactor is heated by an external electric furnace. The temperature distribution was tested, showing that the constant temperature zone of the main reaction area is more than 200 mm high, thus allowing the pyrolysis experiments to be carried out isothermally.

For each run, the furnace temperature was set at a desired value from 700 to 1000 °C. The high-purity (99.999%) carrier gas (N_2 or CO_2) was controlled by a mass flowmeter at a flow rate of 2 L/min and was introduced into the bottom section. When the flow field and the temperature distribution of the reactor were stabilized, coal samples of ~0.2 g were fed downward into the conical section within 10 s, by a casing tube at the top of the reactor. After pyrolysis proceeded for 3 min, the gas flow was immediately cut off and the char particles were allowed to drop into the collection bottle at the bottom. The chars were then collected for further characterization.

The GASMET FTIR Dx4000 gas analyzer was connected to the reactor outlet for online monitoring of the gases released during pyrolysis. To avoid secondary reactions and potential condensing, the sampling line of the gas analyzer was maintained at 180 °C. In addition, a filter containing silica desiccant was placed between the outlet of the reactor and the inlet of the sampling line. The IR absorption band of the analyzer was in the range of 900−4200 cm^{-1}, and the resolution of the spectra was 8 cm^{-1}. The measurement time interval of FTIR spectroscopy was 2 s, and the gas concentrations were determined through processing of the spectra by Calcmet software. To confirm the uncertainty quantification of the experimental results, experiments were repeated and the relative standard deviations of both HCN and NH_3 yields were within 6%.

The HCN or NH_3 yield, which is the ratio of fuel N released as HCN or NH_3, respectively, to the nitrogen in the parent coals, is calculated by the integral of its concentration over time as follows:

$$f_i = \frac{Q\int c_i\,dt}{10^6 \times 22.4\ \text{L/mol}}\frac{M}{mW} \quad (1)$$

where f_i is the yield of i species (HCN or NH_3), Q is the gas flow rate (L/s), c_i is the concentration of i species (ppm), t is the time (s), M is the molecular weight of nitrogen (g/mol), m is the mass of coal (g), and W is the weight fraction of nitrogen in coal.

2.3. Char Structural Characterization. The organic functional groups of the chars were recorded with a FTIR spectrometer (Bruker VERTEX 70, Germany) via the KBr pellet method from 400 to 4000 cm^{-1}, with a resolution of 4 cm^{-1}. First, 1 mg samples were completely mixed with 199 mg of KBr and ground in an agate mortar. The FTIR structural parameters, namely, the A factor, H_{ar}/H_{al} and CH_2/CH_3 were calculated from the peak area according to published methods.[8−10] The A factor represents the relative content of aliphatic functional groups in coal or char; H_{ar}/H_{al} is considered the ratio of the aromatic hydrogen quantity to that of aliphatic hydrogens; and CH_2/CH_3 is used to evaluate the aliphatic chain lengths of coal or char and is regarded as the branching index.

$$A\ \text{factor} = A(3000{-}2800\ \text{cm}^{-1})/[A(3000{-}2800\ \text{cm}^{-1}) + A(1650{-}1520\ \text{cm}^{-1})] \quad (2)$$

$$H_{ar}/H_{al} = A(900{-}700\ \text{cm}^{-1})/A(3000{-}2800\ \text{cm}^{-1}) \quad (3)$$

$$CH_2/CH_3 = A(2920\ \text{cm}^{-1})/A(2950\ \text{cm}^{-1}) \quad (4)$$

XRD analysis of chars was performed by a PANalytical X'Pert PRO X-ray diffractometer with a Cu target and Kα radiation (40 kV and 40 mA). Intensity was recorded from 5° to 65° with a scanning speed of 13.2°/min. The crystallite structural parameters, including interlayer spacing (d_{002}), crystallite diameter (L_a), and average stacking height (L_c), were derived according to Bragg's equation and Scherrer's formula[11]

$$d_{002} = \lambda/(2\sin\theta_{002}) \quad (5)$$

$$L_c = \frac{0.9\lambda}{B_{002}\cos\theta_{002}} \quad (6)$$

$$L_a = \frac{1.84\lambda}{B_{100}\cos\theta_{100}} \quad (7)$$

where λ is the wavelength of the radiation used, B_{002} and B_{100} are the full width at half maximum values of the (002) and (100) peaks, respectively, and θ_{002} and θ_{100} are the corresponding scattering angles at the peak positions.

3. RESULTS AND DISCUSSION

3.1. NO_x Precursor Releasing Profiles under Different Atmospheres. The HCN and NH_3 releasing profiles of EH under different atmospheres are shown in Figure 2. When EH is pyrolyzed at 700 °C in N_2, some HCN but nearly no NH_3 is

DOI: 10.1021/acs.energyfuels.5b01509
Energy Fuels 2015, 29, 7474−7482

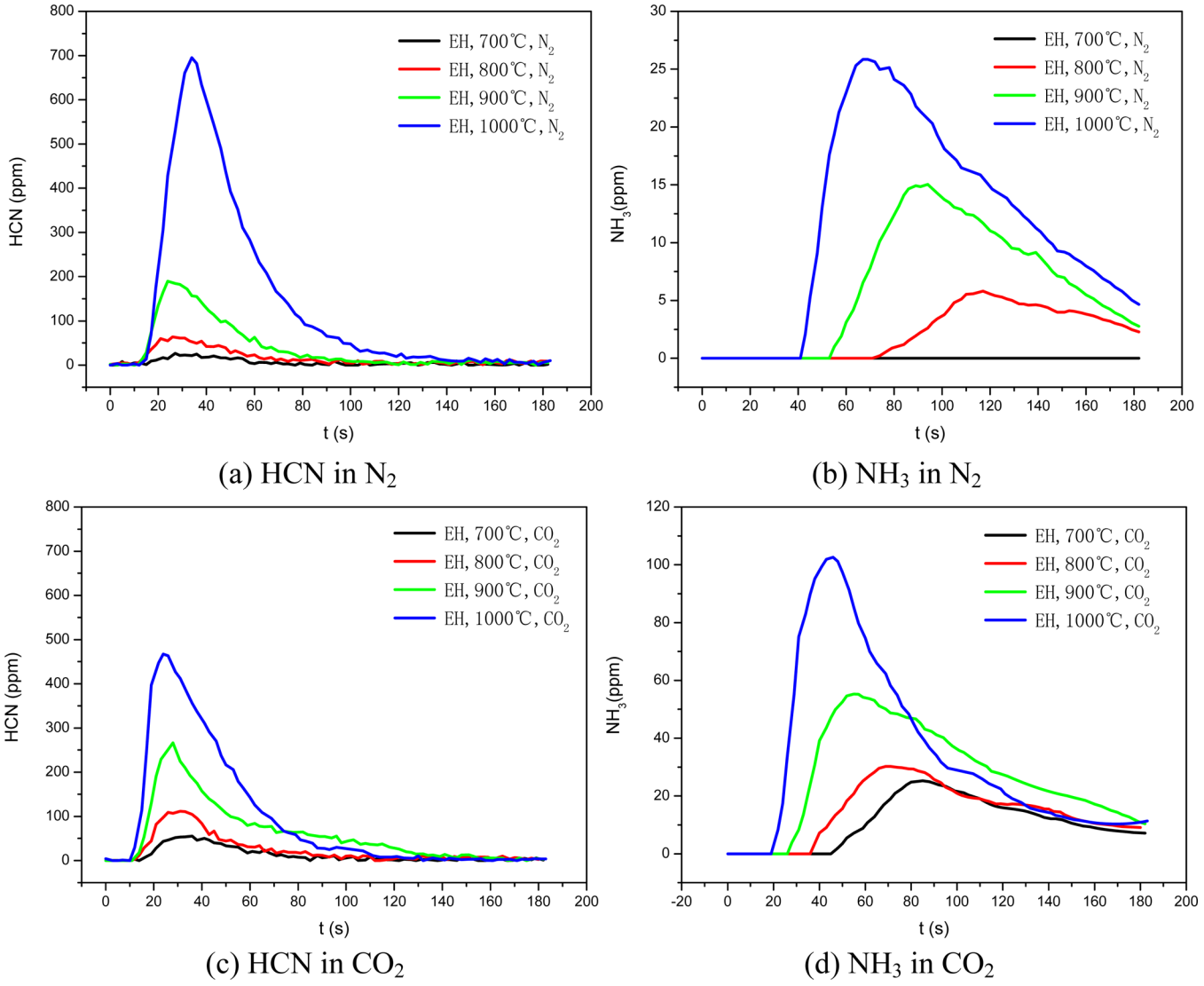

Figure 2. NO_x precursor releasing profiles of EH under N_2 or CO_2.

generated. As the temperature increases from 700 to 1000 °C, the HCN and NH_3 peaks both increase; the HCN peak, in particular, increases considerably above 900 °C. This is consistent with the results of another study.[12] The conversion of pyrrolic or pyridinic nitrogen to nitrile (−CN) groups appears at temperatures higher than 700 °C, and HCN may be generated with the reaction of H radicals and −CN groups.[13] As the temperature reaches 900 °C, the decomposition of N-containing heteroaromatic rings becomes obvious and −CN groups are formed in great quantities, resulting in a large amount of HCN produced. It can be observed that even at the end of pyrolysis, NH_3 continues to be released. This is explained because HCN originates from thermally unstable N-containing structures, whereas NH_3 is produced by the slow conversion of thermally more stable N-containing structures, leading to a much longer formation period for NH_3 than HCN.[14]

As mentioned, the release of NH_3 increases as the pyrolysis temperature increases from 700 to 1000 °C. This differs from the literature, in which the optimal temperature for NH_3 generation was 800 °C, and NH_3 decomposed at a temperature higher than 800 °C, especially in the catalysis of quartz sand or metal.[7,15] However, here, the suspension-bed reactor is made of quartz and no catalyst exists in the reactor; therefore, the decomposition of NH_3 is weak. Furthermore, more H radicals are created and more thermally stable N-containing groups are cracked, enhancing the generation of NH_3 as the temperature increases.

It is noteworthy that the release of NH_3 occurs later than that of HCN and the delay time shortens as the temperature increases. Generally, NH_3 is formed in three ways.[16] First, NH_3 is directly released from the amino groups and amides in low-rank coals. Second, it is associated with the presence of quaternary nitrogen. Third, NH_3 is formed through the hydrogenation of HCN on the surface of nascent char. As shown in Figure 2, almost no NH_3 is released at 700 °C and NH_3 is generated later than HCN above 700 °C, both indicating that NH_3 is not formed directly from the amino groups and amides, which are easily broken at low temperatures. Zhang et al.[17] pointed out that the mechanism of NH_3 formation from HCN hydrogenation on a particular surface is not very convincing, and Li et al.[14] held a similar opinion. Here, when NH_3 is continually generated during the late stage of pyrolysis, no HCN is detected. This also indicates that NH_3 might not originate from the indirect reaction associated with HCN, rather from the slow hydrogenation of thermally stable

DOI: 10.1021/acs.energyfuels.5b01509
Energy Fuels 2015, 29, 7474−7482

N-containing groups with H radicals, such as quaternary nitrogen.[17,18] The formation rate of quaternary N from pyrrolic N and pyridinic N is very low, which leads to a delayed release of NH_3 compared with that of HCN. As the temperature increases, the conversion of quaternary N is accelerated and NH_3 release is enhanced. It should be mentioned that two types of quaternary N might exist, denoted here as thermally unstable quaternary N and thermally stable quaternary N.[19] The former, which mainly exists in low-rank coals and is correlated with oxygen groups, may decompose to form NH_3 at a lower temperature.[17] The latter, which forms from the condensation of polynuclear aromatic structures with little oxygen, is believed to be the important intermediate for NH_3 formation.

The HCN releasing profile of EH under a CO_2 atmosphere is shown in Figure 2c. From 700 to 900 °C, the HCN concentration peaks under CO_2 are higher than under N_2. According to the CO release profiles in Figure 3a, the

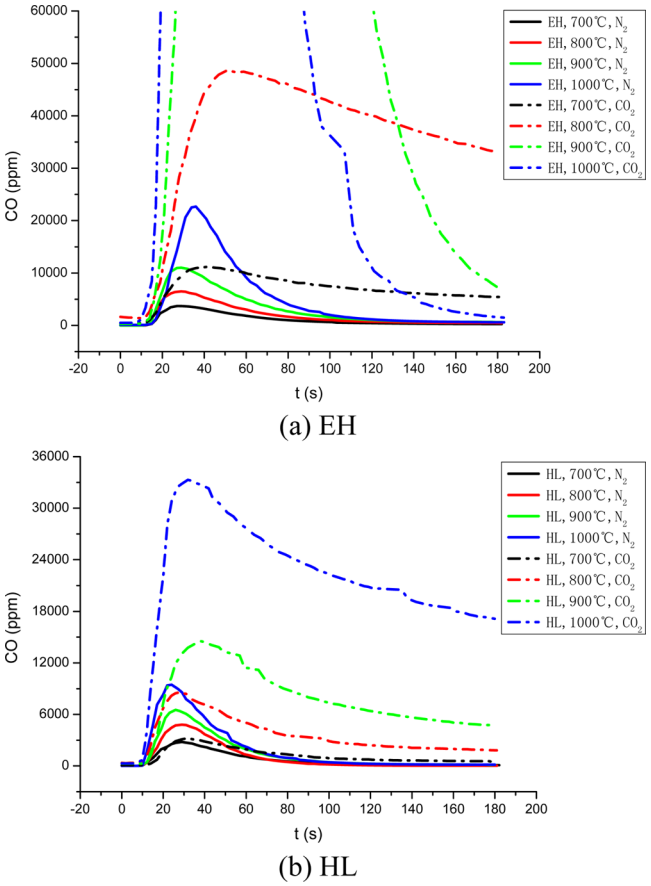

Figure 3. CO releasing profiles of EH and HL under different atmospheres.

gasification of EH char by CO_2 is very strong, even at 700 °C. This may occur because CO_2 gasification breaks the stable −CN groups and exposes them on the char surface. The exposed −CN groups then react with H radicals to form HCN.[6,7] However, at temperatures over 1000 °C, HCN might be oxidized by CO_2, which results in the amount of HCN generated under CO_2 being lower than under N_2.[3]

Figure 2d shows the NH_3 releasing profile of EH in CO_2, which is similar to that under N_2, although in CO_2, NH_3 is produced earlier and the NH_3 peak values are much higher. This result is quite different from that of Duan et al.,[7] in which char CO_2 gasification was not very strong. CO_2 may play completely different roles under different conditions. When char CO_2 gasification is weak, CO_2 might suppress the formation of NH_3 with a blocking effect, but when gasification plays the main role, more H radicals are created, thermally stable N-containing structures are broken, and more NH_3 is formed.[5] Furthermore, some studies[3,5,20] have suggested that if the temperature is high enough, NH_3 can also react with CO_2, as confirmed by Mendiara et al.[21]

The releasing profiles of the NO_x precursors from HL are similar to those from EH; the biggest difference is the releasing concentration, which is related to the characteristics of the coals, such as coal rank, existing forms of N-containing structures, etc. The differences in the amounts of NO_x precursors released from different coals will be investigated in the next section.

3.2. Nitrogen Conversion in Different Atmospheres.

The HCN and NH_3 yields of EH and HL under different atmospheres are shown in Figure 4. It can be observed that the HCN and NH_3 yields of both EH and HL increase as the temperature increases, regardless of the atmosphere (N_2 or CO_2). This might occur because more N-containing groups are broken and more H free radicals are created. Under N_2 atmosphere, the trends of the HCN and NH_3 yields of EH with the change of temperature are nearly the same as those of HL; however, there are notable differences between EH and HL in the CO_2 atmosphere. For both coals, the NH_3 yields in CO_2 are greater than those in N_2, and under most conditions, CO_2 can enhance the production of HCN, except for EH at high temperature (1000 °C) and HL at low temperatures (700 and 800 °C).

For EH coal, the promotion effect of CO_2 on HCN release is enhanced as the temperature increases from 700 to 900 °C. However, with a further temperature increase to 1000 °C, the CO_2 atmosphere greatly reduces the production of HCN. Figure 3a shows that char gasification is obvious for EH pyrolysis/gasification in CO_2 at 700 °C. However, because the temperature is not high enough for the formation of −CN groups through the cracking of thermally unstable N-containing structures, the promotion effect of CO_2 on HCN is not very notable. As the pyrolysis temperature increases, increasingly more −CN groups will be created and the gasification of EH char with CO_2 also becomes stronger, which results in a greater discrepancy between the HCN yields in CO_2 versus N_2. At 1000 °C, the direct reaction of HCN with CO_2 may be significant and part of the HCN produced will be consumed, which leads to a lower HCN yield of EH in CO_2 than in N_2.[3] Furthermore, thermally unstable N-containing structures and −CN groups may also be directly oxidized by CO_2 to produce N_2 prior to the formation of HCN by hydrogenation.

According to the CO release profiles of HL shown in Figure 3b, the gasification of HL char with CO_2 is weak during HL coal pyrolysis/gasification under CO_2 at 700 °C. At low temperature, CO_2 can be adsorbed onto the HL nascent char surface, consuming H radicals and blocking the access of H radicals to N sites,[5,7] causing less HCN to be produced. As temperature increases, the blocking effect is weakened and the gasification of HL char becomes stronger, which enhances the formation of HCN; although at very high temperature (1000 °C), HCN might react with CO_2 directly. Consequently, the promotion effect of CO_2 on the release of HCN is weakened.

Panels b and d of Figures 4 both show that CO_2 can enhance the production of NH_3 because of the gasification of CO_2 with

DOI: 10.1021/acs.energyfuels.5b01509
Energy Fuels 2015, 29, 7474−7482

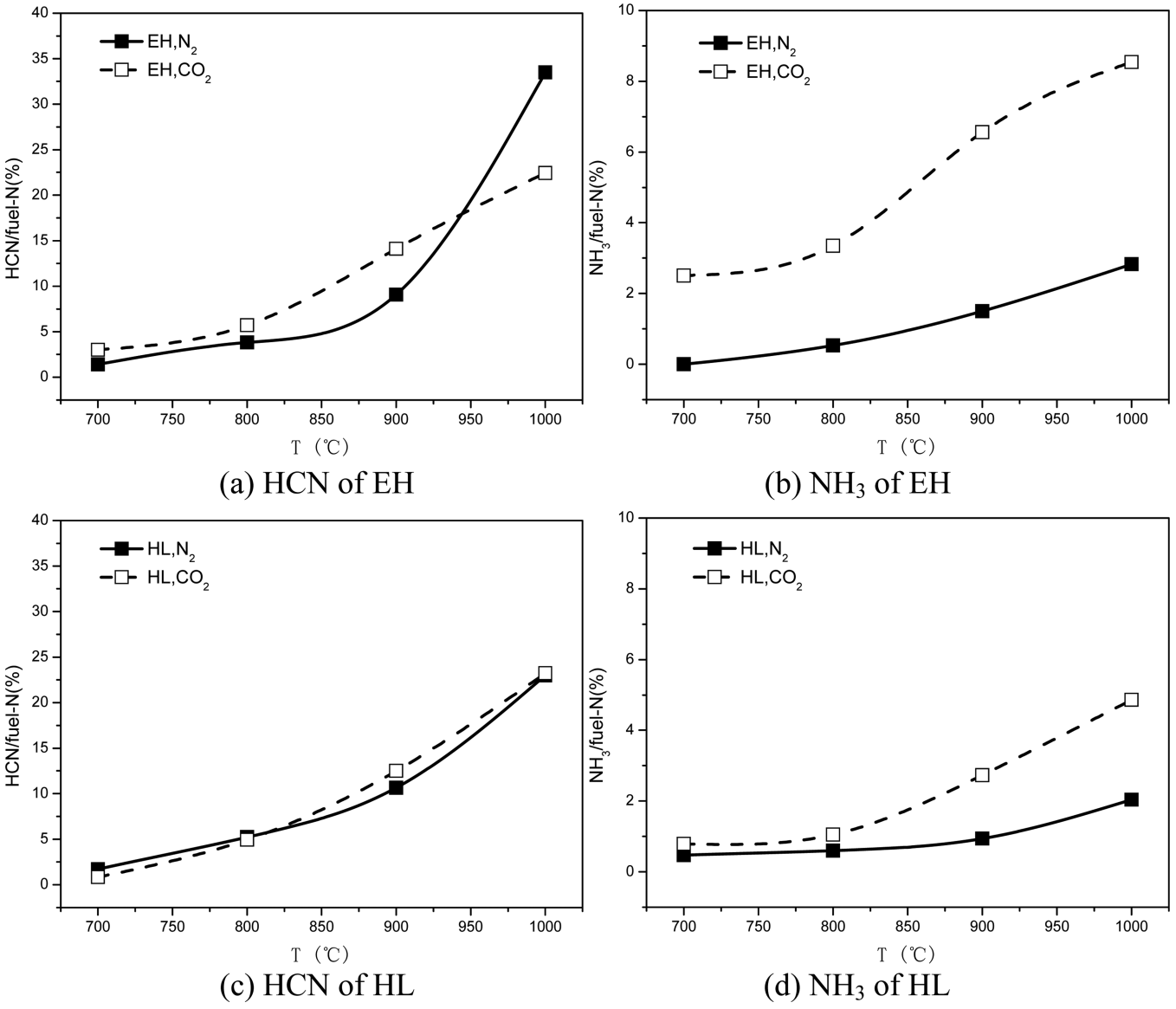

Figure 4. NO_x precursor yields of EH and HL under different atmospheres.

char. However, in comparison to EH coal, the promotion of NH_3 production by CO_2 for HL pyrolysis/gasification at 700 °C is not obvious, because char CO_2 gasification for HL coal at 700 °C is quite difficult. This further confirms the importance of the gasification intensity on the promotion of NH_3 release.

To determine the effect of CO_2 on the selectivity of fuel N conversion to NO_x precursors, the NH_3/HCN ratios are compared in N_2 and CO_2, as shown in Figure 5. The NH_3/HCN molar ratios of both coals in N_2 are much less than 1, which means that HCN is the main NO_x precursor in rapid pyrolysis, in agreement with Glarborg et al.[16] In CO_2 atmosphere, the NH_3/HCN ratios of both coals are greater than those in N_2. This might be attributed to the gasification of CO_2 with char steadily generating H radicals and continuously breaking quaternary N during the late stage of pyrolysis/gasification, which is more beneficial to the formation of NH_3. For EH coal, the difference between the NH_3/HCN ratios under different atmospheres is much greater than that of HL coal. The most important reason for this is that the gasification rate of EH char is much higher than that of HL char.

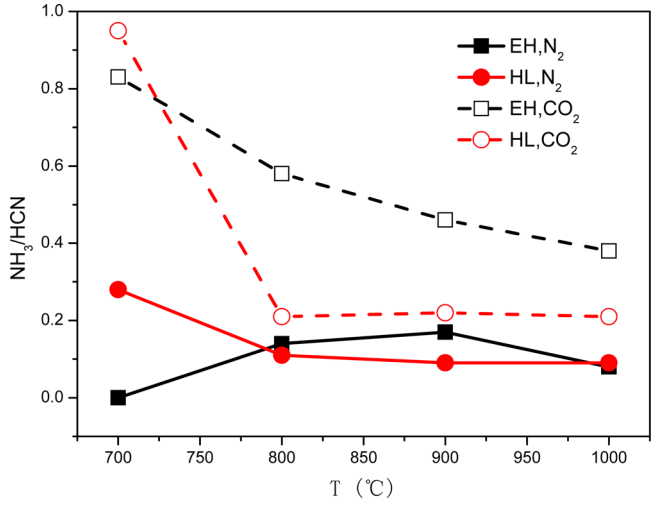

Figure 5. NH_3/HCN ratios of EH and HL under N_2 or CO_2.

DOI: 10.1021/acs.energyfuels.5b01509
Energy Fuels 2015, 29, 7474−7482

3.3. Char Chemical and Physical Structure Evolution during Pyrolysis.

Figure 6 illustrates the FTIR absorption spectra of EH coal and EH chars pyrolyzed in a N_2 atmosphere, in which the absorption peaks of the functional groups are marked. The corresponding functional groups of the absorption bands have been summarized in the literature.[8,9,22] Figure 6 shows that the absorptions of −OH, aliphatic C−H, C═O, and C═C in EH chars decrease significantly with the pyrolysis temperature increasing. This suggests that most of the O-containing groups and many aliphatic chains are broken and removed to form gas products, such as H_2O, CO, CO_2, CH_4, and H_2. In addition, graphitization of char becomes more severe. To study the effects of temperature and CO_2 on H functional groups and the structural evolution of chars during pyrolysis, the FTIR structural parameters (*A* factor, H_{ar}/H_{al} and CH_2/CH_3) were calculated according to eqs 2−4, as shown in Figure 7. It is noteworthy that before calculating the CH_2/CH_3 ratio, the spectral region at 3000−2800 cm^{-1} was curve-fitted by five Gaussian peaks to derive $A(2920\ cm^{-1})$ and $A(2950\ cm^{-1})$, which represent the functional groups of CH_2 and CH_3, respectively.

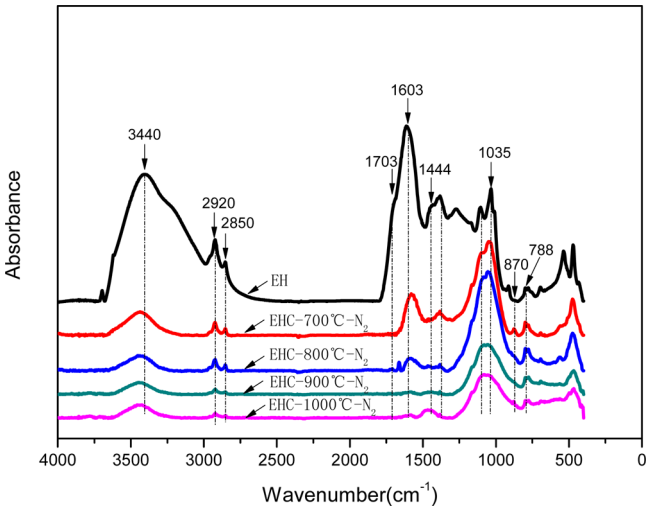

Figure 6. FTIR absorption spectra of EH coal and chars pyrolyzed in N_2 at different temperatures.

For EH coal, the *A* factor value for chars pyrolyzed in N_2 increases with increasing temperature from 700 to 900 °C, which means more aliphatic chains remain in the chars because of the intense reaction of aliphatic fragments with nascent char. This is identical to the CH_4 yield results in Figure 8. However, as the temperature increases further to 1000 °C, the *A* factor decreases. This might occur because the breaking of aliphatic chains is intensive and the condensation becomes more severe. In addition, plenty of H is broken from the aliphatic chains to form H_2. In the CO_2 atmosphere, the *A* factor values of EH chars are less than those under N_2, showing that fewer aliphatic chains remain in the chars. Because the gasification of EH char with CO_2 is evident at 700 °C, CO_2 easily reacts with aliphatic chains, consuming a large amount of $-CH_2$ and $-CH_3$.

For HL chars prepared in N_2, the *A* factor increases as the temperature increases from 700 to 800 °C and then decreases from 800 to 1000 °C, which is similar to that of EH char prepared under N_2. In comparison to the HL chars generated in a N_2 atmosphere, the *A* factor values of chars are promoted by the presence of CO_2, showing that CO_2 is helpful in retaining the aliphatic chains in chars. This phenomenon is contrary to the result of EH chars, which suggests that the effects of CO_2 on the *A* factors for EH chars and HL chars are quite different. This will be discussed further in the XRD results.

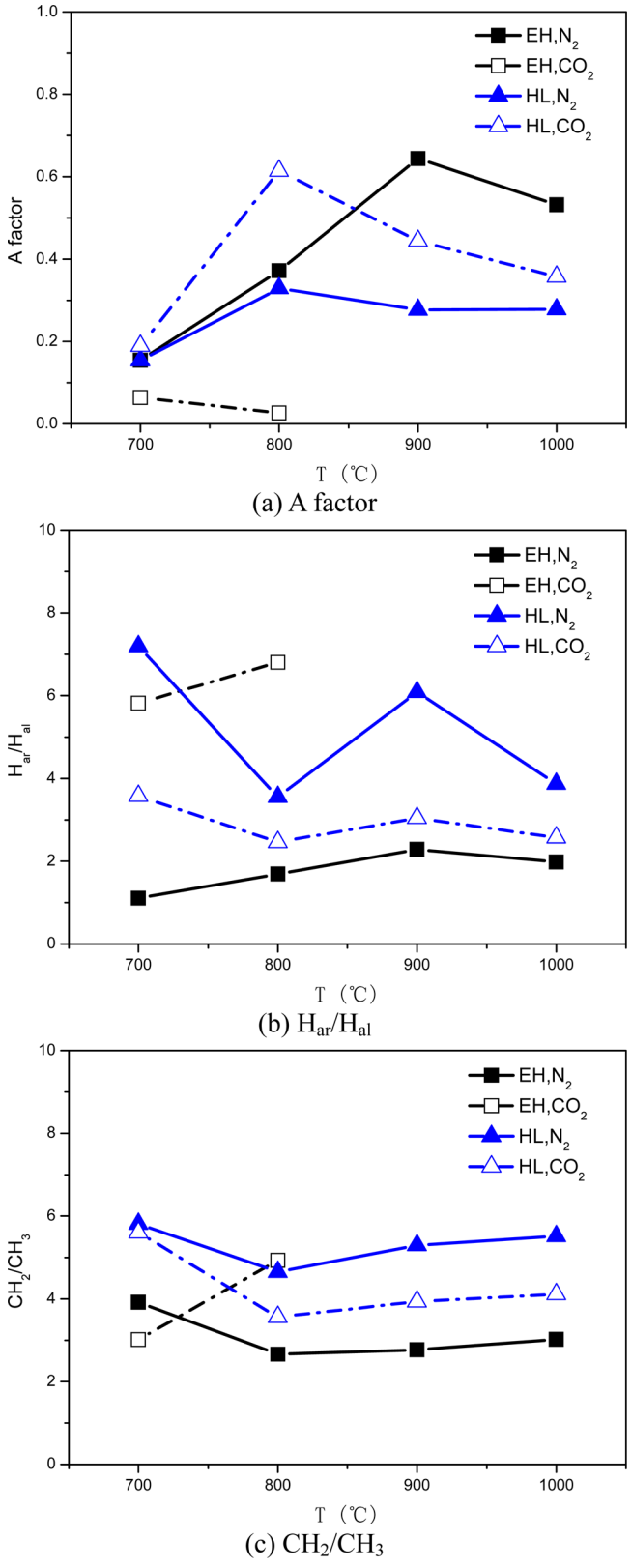

Figure 7. FTIR structural parameters of EH and HL chars under different atmospheres.

DOI: 10.1021/acs.energyfuels.5b01509
Energy Fuels 2015, 29, 7474−7482

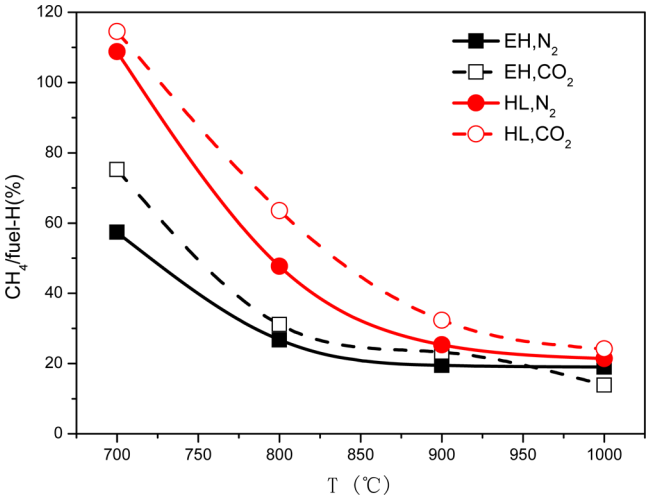

Figure 8. CH_4 yields of EH and HL under N_2 or CO_2.

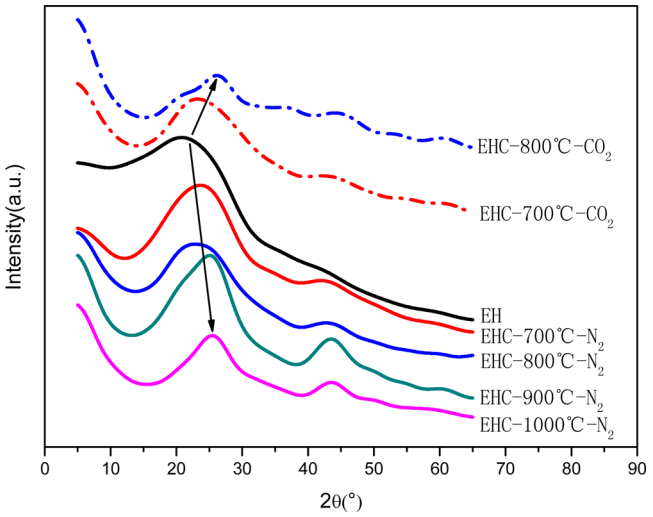

Figure 9. X-ray diffractograms of EH coal and chars.

In Figure 7b, the H_{ar}/H_{al} ratio shows a trend similar to that of the *A* factor. In comparison to the results under N_2 atmosphere, more H is retained as aliphatic chains in HL chars under CO_2 but less H is retained as aliphatic chains in EH chars.

Except for EH in CO_2, the CH_2/CH_3 values of chars decrease from 700 to 800 °C and then increase as the temperature increases further to 1000 °C. Figure 8 shows that with the temperature increasing, the CH_4 yield decreases, which suggests that plenty of $-CH_3$ radicals might be retained in chars, leading to the decrease of CH_2/CH_3. However, as the temperature increases further, the polymerization of char becomes more severe and more $-CH_3$ would take part in the reaction to form $-CH_2$ retained in stable aliphatic chains (such as naphthenic structures), leading to the increase of CH_2/CH_3. It is clear that the char generated in CO_2 shows lower CH_2/CH_3 values than that observed in N_2. This indicates that the aliphatic chain lengths of char derived in CO_2 are shorter than those from the char generated under N_2, which confirms that CO_2 suppresses the polymerization of aliphatic chains. However, EH char pyrolyzed in CO_2 at 800 °C shows a different trend because $-CH_3$ is easier to react with CO_2 than $-CH_2$ and aromatic rings and the char CO_2 gasification is so intense that plenty of $-CH_3$ is consumed. It is impossible to analyze the structures of EH chars prepared under CO_2 at 900 or 1000 °C because the chars were almost completely consumed by the intense gasification.

Figure 9 shows the XRD profiles of EH coal and EH chars. Two obvious peaks are observed in the 2θ ranges of 15−30° and 40−50°, corresponding to a mixed band of μ and (002) peaks and the (100) band, respectively. The μ band arises from saturated structures, such as aliphatic side chains adjacent to coal crystallites, while the (002) and (100) bands are attributed to the stacking structure of aromatic layers and the inplane structure of the aromatics, respectively.[11,23] Thus, the aromaticity (f_a') of char can be defined by eq 8, in which S_{002} and S_μ are the areas of the (002) and μ bands, respectively, representing the ratio of aromatic carbon atoms to the sum of the aromatic and adjacent aliphatic carbon atoms.[23] With the increase of the pyrolysis temperature, the sharpness and intensity of the (002) peak increase and the μ peak gradually disappears.

$$f_a' = \frac{S_{002}}{S_{002} + S_\mu} \tag{8}$$

Two Gaussian peak fittings for the 21° and ∼25° bands are used to deconvolute the mixed peaks in the 2θ range of 10−30° to resolve the (002) peak. The crystallite structural parameters are calculated according to eqs 5−8 and are listed in Table 2.

Table 2. Crystallite Structural Parameters of Coals and Chars

sample	d_{002} (nm)	L_c (nm)	L_a (nm)	f_a'
EH	0.342	1.40	3.56	0.17
EH-700-N_2	0.344	1.34	3.30	0.35
EH-800-N_2	0.345	1.36	3.34	0.39
EH-900-N_2	0.345	1.47	3.64	0.49
EH-1000-N_2	0.349	1.58	3.98	0.68
EH-700-CO_2	0.347	1.08	3.25	0.52
HL	0.352	1.25	6.00	0.54
HL-700-N_2	0.350	1.58	4.09	0.59
HL-700-CO_2	0.357	1.25	3.90	0.52

Because the coal rank of EH is very low, its μ peak is much stronger than its (002) peak. In the N_2 atmosphere, L_c, L_a, and f_a' all increase from 700 to 1000 °C, which means increasingly more aliphatic side chains adjacent to aromatic rings take part in polymerization and the aromatic layers of chars gradually grow as the pyrolysis temperature increases. At 700 °C, L_c and L_a of EH char in N_2 are greater than those in CO_2 but d_{002} and f_a' show different tendencies. This indicates that the gasification of char with CO_2 greatly consumes $-CH_2$ methylene groups and leads to the more disordered structure of char generated in CO_2.

At 700 °C, the differences between the crystallite parameters of HL chars in different atmospheres are similar to those of the EH chars, except for f_a'. This indicates that the size of the aromatic polymers of chars is smaller in CO_2 than in N_2. Unlike EH char, the f_a' value of HL char is reduced by CO_2, showing that more aliphatic chains are retained in the HL char by the effect of CO_2, which agrees with the conclusion from the *A* factors in Figure 7a. It is reasonable to believe that during the process of pyrolysis/gasification, CO_2 could react with aromatic polymers, which would lead to the decrease of crystallite size.

DOI: 10.1021/acs.energyfuels.5b01509
Energy Fuels 2015, 29, 7474−7482

Meanwhile, as the reactivity of aliphatic chains is stronger than that of aromatic rings, aliphatic chains would be consumed much faster than the latter, resulting in the increase of f_a'. However, this does not agree with the HL char result; therefore, this may be caused by some other reasons.

According to the CO releasing concentration in Figure 3, it can be concluded that in CO_2, the reactivity of EH char is much greater than that of HL char. At 700 °C, CO_2 intensively reacts with EH char but very slightly with HL char. It is deduced that when some of the aliphatic chains are broken and condensation of char or tar occurs during pyrolysis in the CO_2 atmosphere, CO_2 could be adsorbed on the char surface and block aliphatic fragments from taking part in condensation. As a result, a considerable amount of H remains in the aliphatic chains of the chars and aromatic polymers cannot develop completely. Therefore, in comparison to chars pyrolyzed in N_2, CO_2 can produce more disordered chars and reduce the size of the aromatic polymers of chars, which is in agreement with the results of others.[24,25] Subsequently, because of the intensive gasification of EH char by CO_2 at 700 °C, CO_2 can react with aliphatic chains and aromatic polymers. The reaction rate of CO_2 with the former is much faster than that of the latter, reducing the size of the aromatic polymers further, and f_a' increases to a higher value than that in N_2.[26] For the HL char pyrolyzed in CO_2 for 3 min, the gasification is so weak that the characterization of the char does not change much at the end of pyrolysis/gasification, causing a lower f_a' than that in N_2.

The combined results of the char characterization and the HCN and NH_3 formation suggest that CO_2 can suppress aliphatic chains taking part in condensation and more H is retained as $-CH_2$ or $-CH_3$ in chars but does not remain in stable aromatic polymers in the initial stage of pyrolysis/gasification. Simultaneously, CO_2 can promote the shedding of H-containing groups and increase the mobility of H free radicals,[26] which leads to the formation of more HCN. With the completion of pyrolysis, CO_2 gasification continues, thermally stable N-containing structures start to break up, and more H free radicals are produced from rich aliphatic chains in chars by gasification. Hence, the formation of NH_3 is promoted. In this process, the gasification of char plays a critical role. With the increase of gasification intensity, the promotion effect of CO_2 on the generation of HCN and NH_3 will be enhanced.

4. CONCLUSION

(1) For both EH lignite and HL bituminous coal, more HCN and NH_3 are produced at higher pyrolysis temperatures. (2) NH_3 might not originate from indirect HCN hydrogenation on a particular surface. Thermally stable quaternary N is believed to be the important intermediate for the formation of NH_3. (3) The effects of CO_2 on the formations of HCN and NH_3 are summarized in four main ways. (a) When char CO_2 gasification is weak at a low temperature, CO_2 can be adsorbed on the char surface and block the access of H radicals to N sites, suppressing the production of HCN. (b) CO_2 can promote the release of H free radicals and the cracking of N-containing groups, which is beneficial to the formation of HCN and NH_3. (c) When the pyrolysis temperature is as high as 1000 °C, the presence of CO_2 suppresses the production of HCN for EH coal, which may occur because part of generated HCN is consumed by the reaction with CO_2. (d) CO_2 can suppress the polymerization of aliphatic chains, and more H is retained as $-CH_2$ or $-CH_3$ in chars during coal pyrolysis. This helps to produce abundant H radicals for the formation of NH_3 in the late stage of pyrolysis/gasification.

AUTHOR INFORMATION

Corresponding Author

*Telephone: +86-27-87542417-8211. Fax: +86-27-87545526. E-mail: shzhang@hust.edu.cn.

Notes

The authors declare no competing financial interest.

ACKNOWLEDGMENTS

The authors really appreciate the financial support of the National Natural Science Foundation of China (51276075 and 51576088) and the National Science and Technology Pillar Program (2011BAC05B03). The authors also thank Analytical and Testing Center, Huazhong Universtiy of Science and Technology, China, for assistance with FTIR spectroscopy and XRD measurement.

REFERENCES

(1) Toftegaard, M. B.; Brix, J.; Jensen, P. A.; Glarborg, P.; Jensen, A. D. Oxy-fuel combustion of solid fuels. *Prog. Energy Combust. Sci.* **2010**, *36* (5), 581−625.

(2) Buhre, B. J. P.; Elliott, L. K.; Sheng, C. D.; Gupta, R. P.; Wall, T. F. Oxy-fuel combustion technology for coal-fired power generation. *Prog. Energy Combust. Sci.* **2005**, *31* (4), 283−307.

(3) Ohtsuka, Y.; Furimsky, E. Effect of ultrafine iron and mineral matter on conversion of nitrogen and carbon during pyrolysis and gasification of coal. *Energy Fuels* **1995**, *9* (1), 141−147.

(4) Feng, J.; Li, W.; Xie, K.; Liu, M.; Li, C. Studies of the release rule of NO_X precursors during gasification of coal and its char. *Fuel Process. Technol.* **2003**, *84* (1−3), 243−254.

(5) Chang, L.; Xie, Z.; Xie, K.; Pratt, K. C.; Hayashi, J.; Chiba, T.; Li, C. Formation of NO_X precursors during the pyrolysis of coal and biomass. Part VI. Effects of gas atmosphere on the formation of NH_3 and HCN. *Fuel* **2003**, *82* (10), 1159−1166.

(6) Duan, L.; Zhao, C.; Zhou, W.; Qu, C.; Chen, X. Investigation on coal pyrolysis in CO_2 atmosphere. *Energy Fuels* **2009**, *23* (7), 3826−3830.

(7) Duan, L.; Zhao, C.; Ren, Q.; Wu, Z.; Chen, X. NO_X precursors evolution during coal heating process in CO_2 atmosphere. *Fuel* **2011**, *90* (4), 1668−1673.

(8) Li, W.; Zhu, Y. Structural characteristics of coal vitrinite during pyrolysis. *Energy Fuels* **2014**, *28* (6), 3645−3654.

(9) Wu, D.; Liu, G.; Sun, R. Investigation on structural and thermodynamic characteristics of perhydrous bituminous coal by fourier transform infrared spectroscopy and thermogravimetry/mass spectrometry. *Energy Fuels* **2014**, *28* (5), 3024−3035.

(10) Ibarra, J.; Muñoz, E.; Moliner, R. FTIR study of the evolution of coal structure during the coalification process. *Org. Geochem.* **1996**, *24* (6−7), 725−735.

(11) Yin, Y.; Zhang, J.; Sheng, C. Effect of pyrolysis temperature on the char micro-structure and reactivity of NO reduction. *Korean J. Chem. Eng.* **2009**, *26* (3), 895−901.

(12) Li, C.; Nelson, P. F.; Ledesma, E. B.; Mackie, J. C. An experimental study of the release of nitrogen from coals pyrolyzed in fluidized-bed reactors. *Symp. (Int.) Combust., [Proc.]* **1996**, *26* (2), 3205−3211.

(13) Li, C.; Buckley, A. N.; Nelson, P. F. Effects of temperature and molecular mass on the nitrogen functionality of tars produced under high heating rate conditions. *Fuel* **1998**, *77* (3), 157−164.

(14) Li, C.; Tan, L. Formation of NO_X and SO_X precursors during the pyrolysis of coal and biomass. Part III. Further discussion on the formation of HCN and NH_3 during pyrolysis. *Fuel* **2000**, *79* (15), 1899−1906.

(15) Tan, L.; Li, C. Formation of NO_X and SO_X precursors during the pyrolysis of coal and biomass. Part II. Effects of experimental

DOI: 10.1021/acs.energyfuels.5b01509
Energy Fuels 2015, 29, 7474−7482

conditions on the yields of NO_X and SO_X precursors from the pyrolysis of a Victorian brown coal. *Fuel* **2000**, *79* (15), 1891−1897.
(16) Glarborg, P.; Jensen, A. D.; Johnsson, J. E. Fuel nitrogen conversion in solid fuel fired systems. *Prog. Energy Combust. Sci.* **2003**, *29* (2), 89−113.
(17) Zhang, H.; Fletcher, T. H. Nitrogen transformations during secondary coal pyrolysis. *Energy Fuels* **2001**, *15* (6), 1512−1522.
(18) Kambara, S.; Takarada, T.; Yamamoto, Y.; Kato, K. Relation between functional forms of coal nitrogen and formation of nitrogen oxide (NO_X) precursors during rapid pyrolysis. *Energy Fuels* **1993**, *7* (6), 1013−1020.
(19) Kelemen, S. R.; Gorbaty, M. L.; Kwiatek, P. J.; Fletcher, T. H.; Watt, M.; Solum, M. S.; Pugmire, R. J. Nitrogen transformations in coal during pyrolysis. *Energy Fuels* **1998**, *12* (1), 159−173.
(20) Jones, J. M.; Harding, A. W.; Brown, S. D.; Thomas, K. M. Detection of reactive intermediate nitrogen and sulfur species in the combustion of carbons that are models for coal chars. *Carbon* **1995**, *33* (6), 833−843.
(21) Mendiara, T.; Glarborg, P. Ammonia chemistry in oxy-fuel combustion of methane. *Combust. Flame* **2009**, *156* (10), 1937−1949.
(22) Ibarra, J.; Moliner, R.; Bonet, A. J. FT-i.r. investigation on char formation during the early stages of coal pyrolysis. *Fuel* **1994**, *73* (6), 918−924.
(23) Wu, D.; Liu, G.; Sun, R.; Fan, X. Investigation of structural characteristics of thermally metamorphosed coal by FTIR spectroscopy and X-ray diffraction. *Energy Fuels* **2013**, *27* (10), 5823−5830.
(24) Bai, Y.; Wang, P.; Yan, L.; Liu, C.; Li, F.; Xie, K. Effects of CO_2 on gas evolution and char structure formation during lump coal pyrolysis at elevated pressures. *J. Anal. Appl. Pyrolysis* **2013**, *104*, 202−209.
(25) Wang, B.; Sun, L.; Su, S.; Xiang, J.; Hu, S.; Fei, H. Char structural evolution during pyrolysis and its influence on combustion reactivity in air and oxy-fuel conditions. *Energy Fuels* **2012**, *26* (3), 1565−1574.
(26) Gao, S.; Zhao, J.; Wang, Z.; Wang, J.; Fang, Y.; Huang, J. Effect of CO_2 on pyrolysis behaviors of lignite. *Journal of Fuel Chemistry and Technology* **2013**, *41* (3), 257−264.

DOI: 10.1021/acs.energyfuels.5b01509
Energy Fuels 2015, 29, 7474−7482